

3D Registration by Using an Alternative 3D Shape Representation

C. TORRE-FERRERO, S. ROBLA, E.G. SARABIA, J.R. LLATA
 Electronics Technology, Systems and Automation Engineering Department
 University of Cantabria
 Av. Los Castros s/n. 39005 Santander
 SPAIN

Abstract: - This paper introduces a surface matching algorithm for 3D registration that uses an alternative 3D Shape Representation: CIRCON (Cylindrical Image of Radial Contours), that both enables the compression of the 3D data, making them more manageable, and facilitates the tasks related to surface matching. By making use of the properties of this 3D shape representation two surfaces whose relative pose is unknown can be aligned. The information obtained by the surface matching process is then used for calculating a coarse transformation (rotation and translation) between both surfaces.

Key-Words: - 3D registration, surface alignment, shape representation, coarse transformation, object recognition.

1 Introduction

In recent years, numerous shape representations have arisen that make a contribution to the 3D registration problem in computer vision. Specifically, the existing surface matching algorithms use either intrinsic or extrinsic surface properties in order to find a correspondence between two surfaces whose relative pose is unknown. The intrinsic properties relate the surface to itself whereas the extrinsic ones relate it to the coordinate frame in which the surface is expressed. Both types of properties give rise to different approaches depending on the chosen characteristics (such as spin images, geometric histogram, surface signatures, harmonic shape images, etc). All these methods extract the 3D shape descriptors from both surfaces in order to compare them. If many correspondences are found, then a coarse transformation that aligns them in a proper way can be calculated.

In the following sections a surface matching process is presented that uses an alternative 3D shape representation. The results provided by this process allow to obtain directly a coarse transformation between the two surfaces.

2 CIRCON: 3D Shape Representation

2.1 3D Shape Representations

Diverse types of coordinates are used by some well-known shape representations in different ways in order to index different geometric properties. Next, a concise description of the most important ones is made. A more complete analysis can be found in [12].

2.1.1 Spin Images

This representation extracts features based on horizontal and perpendicular distances from regions around an interest-point. These features are represented using smoothed 2D histograms known as spin-images [3], [13].

2.1.2 Geometric histograms

The angles between normals and perpendicular distances are extracted as features from the regions. These features are accumulated in smoothed 2D geometric histograms [4], [5].

2.1.3 Surface signatures

This representation uses the whole surface around the interest-point. Distance and angular features are extracted from the region and are represented using 2D signatures [6].

2.1.4 Harmonic shape image

Features based on curvature are extracted from the regions to create 2D representations known as harmonic shape images [7].

Our 3D shape representation is based on cylindrical coordinates, as is explained in the following section.

2.2 Description

As is shown in Fig.1, the generation process of this 3D shape representation can be visualized as a plane that is rotated around the surface normal at one point of the object, producing a slice for each angle θ_i being considered. The contours of these slices are coded and stored in a matrix.

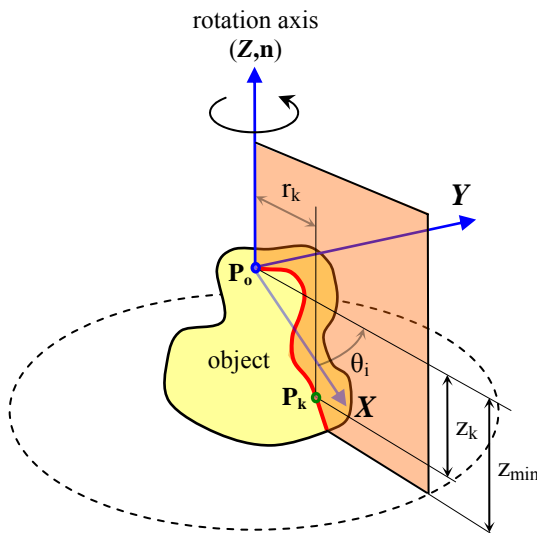


Fig.1. Generation of the 3D shape representation.

If a transformation based on cylindrical coordinates is defined, given a 3D point P_k belonging to a slice i (angle θ_i) and whose Cartesian coordinates are (x_k, y_k, z_k) , these could be transformed by using the following expressions:

$$i = \text{round} \left(\frac{-\tan^{-1} \left(\frac{y_k}{x_k} \right)}{\rho_\theta} + 1 \right) \tag{1}$$

$$j = \text{round} \left(\frac{\sqrt{x_k^2 + y_k^2}}{\rho_r} + 1 \right) \tag{2}$$

$$c_{i,j} = \text{round} \left(\frac{z_k}{\rho_z} \right) \tag{3}$$

where ρ_θ is the angular resolution, ρ_r the radial resolution and ρ_z the height resolution; c_{ij} is the matrix element that belongs to i row and j column.

		radius →				
angle ↓	$c_{1,1}$	$c_{1,2}$...	$c_{1,j}$...	$c_{1,nr}$
	$c_{2,1}$	$c_{2,2}$...	$c_{2,j}$...	$c_{2,nr}$
	⋮	⋮	⋮	⋮	⋮	⋮
	$c_{i,1}$	$c_{i,2}$...	$c_{i,j}$...	$c_{i,nr}$
	⋮	⋮	⋮	⋮	⋮	⋮
	$c_{ns,1}$	$c_{ns,2}$...	$c_{ns,j}$...	$c_{ns,nr}$

Fig. 2. CIRCON matrix. The arrows shown in the figure indicate the increasing direction for angle and radius.

By applying this transformation to all the slices, the results can be stored in a matrix, as is shown in Fig.2. This matrix can be visualized as an image (see Fig.3),

where the row indexes indicate the number of angular section (slice) whereas the columns indexes code the radius and the image grey levels code the heights. The matrix will have $n_s = 2\pi/\rho_\theta$ rows, one for each prefixed rotation angle.



Fig. 3. CIRCON of an alternator cover ($\rho_\theta = 2.5^\circ$, $\rho_r = \rho_z = 0.5\text{mm}$).

2.3 Properties

An example of the resultant image of applying this transformation to the 3D points belonging to an arbitrary pose of an alternator cover is shown in Fig.3. The resolutions being used can be seen in the footnote. According to this, the number of rows is 144.

It is interesting to note that the last and the first rows of the image keep continuity in the grey levels respectively. This is logical since the sequence of slices is closed. Hence, this is a kind of cylindrical image. Moreover, every row represents the object contour belonging to that radial plane (slice).

Consequently, the name we have chosen for this 3D shape representation is CIRCON (Cylindrical Image of Radial CONtours).

This 3D shape representation has the following main properties:

- it is object-centred.
- it can be used for global or local representation.
- it is robust to clutter and occlusion.
- it compress the 3D shape, making it more manageable.
- the shape of the object can be recovered (though sampled).

A more detailed description can be found in [14].

3 Surface Matching

Since the goal of this process is to obtain the best matching between two surfaces S_A and S_B belonging to the same object, a global matching is performed, i.e., the *circon* images are generated using the entire surfaces.

The results obtained by this process are used later for calculating a coarse transformation that aligns both surfaces.

Two views of the same object and its initial misalignment are shown in Fig. 4.

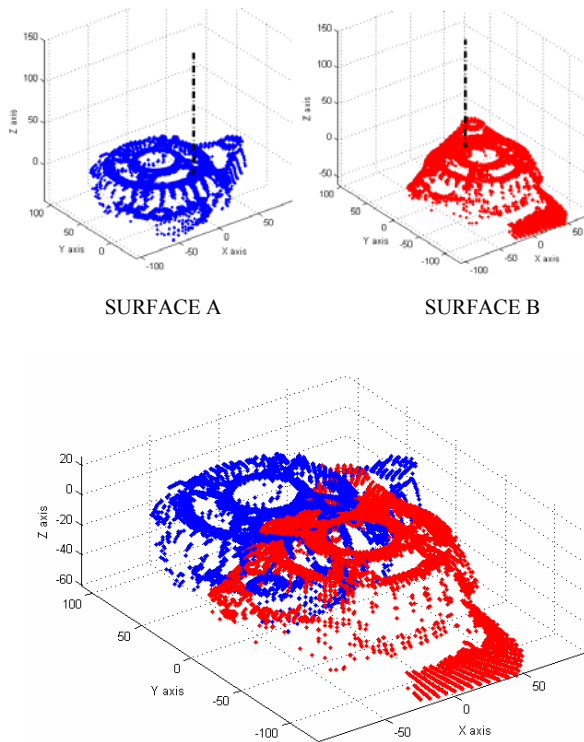


Fig. 4. Initial misalignment.

A block diagram of the surface matching process is shown in Fig. 6, given two *circon* images, *A* and *B*, corresponding to different poses of the same object (see Fig. 5). In order to find a correspondence between their corresponding surfaces, S_A and S_B , will be necessary to transform one of the *circon* images in order to compare them. This transformation is detailed in Section 3.1.



Fig. 5. CIRCON images for two different poses of the same object.

If *A* is transformed, then the resultant *circon* image $A(i_o, j_o)$ is compared with *B* by using a similarity measure explained in Section 3.2. The measure obtained M_s is stored and a new iteration is performed.

When a sufficient number of indexes has been proved, then the ten transformed *circon* images with the highest similarity measures are chosen for verifying which of them produces the best alignment between the two surfaces S_A and S_B (Section 3.3).

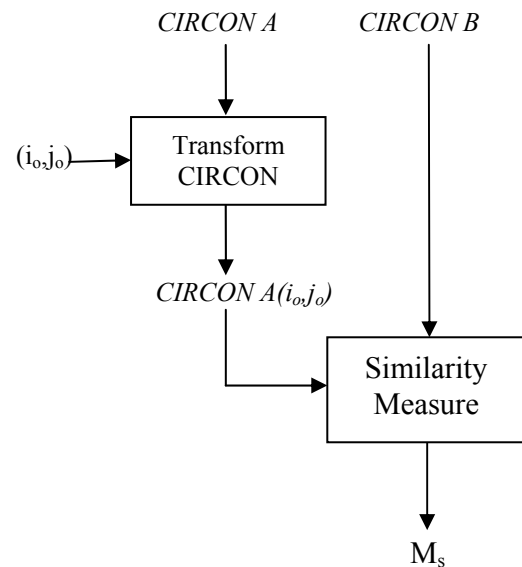


Fig. 6. Block diagram of the surface matching

3.1 Transformation of a CIRCON

In order to find a correspondence between the two surfaces, a transformation of one of the two corresponding *circon* images has to be performed. This transformation modifies the original *circon*, producing a new one that will be compared with the other *circon*.

Suppose that, as is shown in Fig. 6, *circon A* is to be transformed. If two indexes (i_o, j_o) are provided, this transformation modifies all the matrix elements and their original positions by centering the *circon* in the 3D point corresponding to the pixel with row index i_o and column index j_o in the image.

The transformation comprises three steps. Firstly, the following expressions are applied to all the pairs (i, j) in the matrix.

$$x'_{ij} = \rho_r \cdot (j \cdot \cos(\rho_\theta \cdot (i-1)) - j_o \cdot \cos(\rho_\theta \cdot (i_o-1))) \quad (4)$$

$$y'_{ij} = -\rho_r \cdot (j \cdot \sin(\rho_\theta \cdot (i-1)) + j_o \cdot \sin(\rho_\theta \cdot (i_o-1))) \quad (5)$$

The new position (i', j') of the pixel a_{ij} will be calculated by (1) and (2), whereas the pixel value by,

$$c_{i'j'} = c_{ij} - c_{i_o j_o} \quad (6)$$

The next step will be to refer the new *circon* to the surface normal at the 3D point where it is centered now. The normal is calculated by fitting a plane to the 3D points obtained from the neighboring pixels. Hence, the data from the matrix will be rotated by using the following matrix:

$$R_n = [\bar{x}_n \quad \bar{n} \times \bar{x}_n \quad \bar{n}]^T, \quad (7)$$

where

$$\bar{x}_n = \frac{[0 \ 1 \ 0]^T \times \bar{n}}{\|[0 \ 1 \ 0]^T \times \bar{n}\|} \quad (8)$$

Finally, the last k rows will be moved to the beginning of the matrix. This produces, since the image is cylindrical, a counter-clockwise rotation about the surface normal of ρz - k radians.

The resultant matrix of applying these three steps will be denoted by $A(i_o, j_o)$.

3.2 Similarity Measure

Before any calculation is made, the minimum values of both matrices ($A(i_o, j_o)$ and B) have to be equal.

Let the minimum of both matrices be

$$m = \min(A(i_o, j_o), B) \quad (9)$$

Hence, if $a_{ij} = \min(A)$ then $a_{ij} = m$. In the same way, if $b_{ij} = \min(B)$ then $b_{ij} = m$.

Then, the similarity measure is defined as

$$M_s = \frac{\sum_i \sum_j^{n_r} (a_{ij} - \bar{A})(b_{ij} - \bar{B}) \cdot w_{ij}}{\sqrt{\left(\sum_i \sum_j^{n_r} (a_{ij} - \bar{A})^2 \cdot w_{ij} \right) \left(\sum_i \sum_j^{n_r} (b_{ij} - \bar{B})^2 \cdot w_{ij} \right)}} \quad (10)$$

where the mean values \bar{A} and \bar{B} are given by

$$\bar{A} = \frac{1}{n_s \cdot n_r} \sum_i \sum_j^{n_r} a_{ij} \quad (11)$$

and

$$\bar{B} = \frac{1}{n_s \cdot n_r} \sum_i \sum_j^{n_r} b_{ij} \quad (12)$$

This is a weighted correlation coefficient. The weights are assigned to be the column index of the pixel being evaluated in both images. Therefore, both a pixel a_{ij} and b_{ij} will have a weight $w_{ij} = j$. In this way, the pixels far from the central point are better weighted, since they represent a larger area of the object. However, if $a_{ij} = m$ and $b_{ij} = m$ then $w_{ij} = 0$. Furthermore, if $a_{ij} = m$ and $b_{ij} \neq m$ (or vice versa), then

$$w_{ij} = j \cdot \left(1 - \frac{\sum_{(i,j) \in I} w_{ij}}{\sum_{(i,j) \in U} w_{ij}} \right) \quad (13)$$

where I and U are respectively the intersect set and the union set of indexes defined as

$$I = \{(i, j) \mid (a_{ij} \neq m) \text{ and } (b_{ij} \neq m)\} \quad (14)$$

$$U = \{(i, j) \mid (a_{ij} \neq m) \text{ or } (b_{ij} \neq m)\} \quad (15)$$

3.3 Verification of the best matches

Once a sufficient number of indexes has been proved, the ten transformed *circon* images with the highest similarity measures are chosen for verification. An example is shown in Fig. 7. The first image corresponds to the original *circon* A , whereas the ten next ones are its transformed *circon* images $A(i_o, j_o)$ with the highest M_s . The last one corresponds to *circon* B , the image that they were compared with.

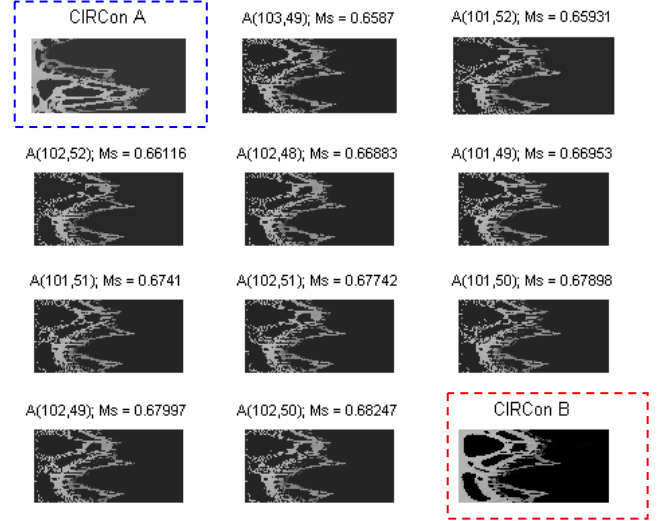


Fig. 7. The ten *circon* images with the highest similarity

The following expression is evaluated for each of these ten images:

$$M_d = \frac{tol}{\sum_i \sum_j^{n_r} w_{ij}} \left(\sum_i \sum_j^{n_r} \frac{w_{ij}}{\max\{|a_{ij} - b_{ij}| - d_w, tol\}} \right) \quad (16)$$

This allows to verify if the distance between both surfaces is sufficiently small and to determine which of the *circon* images provides the best alignment.

The values of M_d are comprised between 0 and 1. If both images were exactly equal, then $M_d = 1$.

Note that the pairs of pixels whose distances are smaller than $d_w + tol$ will have a weight equal to $1/tol$, whereas the weights for the rest will be inversely proportional to the distance between both pixels. Accordingly, this formula gives a higher importance to the pixels whose distance is very small. In the verification results shown in Table I, $d_w = 1$ and $tol = 0.1$.

Table 1
 VERIFICATION RESULTS

<i>circon</i>	M_s	M_d
A(102,52)	0.65265	0.1376
A(103,50)	0.65455	0.1374
A(103,49)	0.65693	0.1359
A(101,49)	0.66673	0.1462
A(102,48)	0.66949	0.1420
A(101,51)	0.67117	0.1426
A(102,51)	0.67648	0.1397
A(101,50)	0.6786	0.1441
A(102,49)	0.68284	0.1432
A(102,50)	0.68495	0.1440

The *circon* with the highest M_d will be considered that produces the best alignment between the two surfaces S_A and S_B . In Table 1, A(101,49) has $M_d=0.1462$, i.e., the best alignment is produced when indexes are $i_s=101, j_s=49$. In this case $k_s=70$.

4 3D Registration

One interesting property of this 3D representation is that, once the best correspondence is determined, the 3D transformation between both surfaces depends on the indexes (i_s, j_s) and the number of columns k_s that were moved when Ai_{j_s} was generated.

The two following expressions are necessary to calculate the transformation (translation vector and rotation matrix) that align both surfaces S_A and S_B .

Translation vector:

$$t(i_s, j_s) = \begin{pmatrix} \rho_r \cdot j_s \cdot \cos(-\rho_\theta \cdot (i_s - 1)) \\ \rho_r \cdot j_s \cdot \sin(-\rho_\theta \cdot (i_s - 1)) \\ \rho_z \cdot a_{ij} \end{pmatrix} \quad (17)$$

Rotation matrix:

$$R(i_s, j_s, k_s) = R_z(k_s) \cdot R_n \quad (18)$$

where R_n is the matrix obtained in (7) and,

$$R_z(k_s) = \begin{pmatrix} \cos(\rho_\theta \cdot k_s) & \sin(\rho_\theta \cdot k_s) & 0 \\ -\sin(\rho_\theta \cdot k_s) & \cos(\rho_\theta \cdot k_s) & 0 \\ 0 & 0 & 1 \end{pmatrix} \quad (19)$$

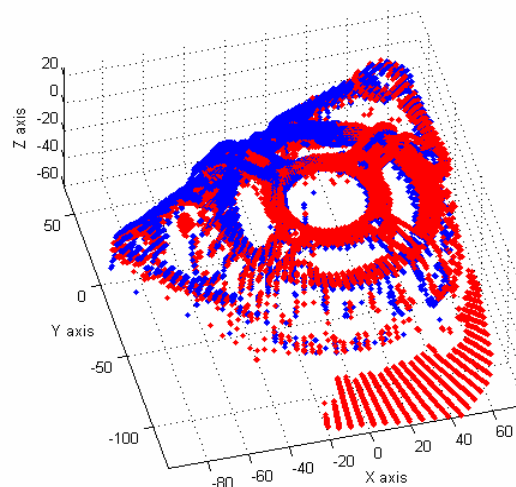
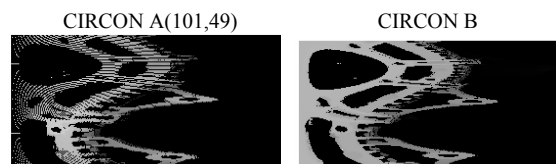


Fig. 8. Final alignment

As is shown in Fig.8, the coarse transformation obtained is sufficiently good and it can be used as an initial estimate by the ICP algorithm [1],[2] if a finer alignment is required.

5 Conclusion

A surface matching algorithm for 3D registration has been presented in this paper. This algorithm makes use of an alternative 3D shape representation that allows the characterization of 3D objects by means of a matrix where the radial contours are coded and stored by rows. As has been shown, this representation can prove very useful for accomplishing diverse tasks in 3D computer vision.

At the present time we are working on developing new algorithms for 3D registration and object recognition by using different techniques based on artificial intelligence. At this moment we have obtained the first results by using a wavelets-based algorithm that reduces the execution time to a few seconds. Our goal is to improve this algorithm for coping with the tasks presented in this paper in an efficient and effective way.

References:

- [1] P.J. Besl, N.D. McKay, "A method of registration of 3-D shapes", *IEEE Trans. Pattern Anal. Mach. Intell.* 14 (2) (1992) 239–256.

- [2] Y. Chen, G. Medioni, "Object modeling by registration of multiple range images", *Image Vision Comput.* 10 (3) (1992) 145–155.
- [3] A. Johnson, M. Hebert, "Using spin images for efficient object recognition in cluttered 3D scenes", *IEEE Trans. Pattern Anal. Mach. Intell.* 21 (5) (1999) 433–449.
- [4] A. Ashbrook, R. Fisher, N. Werghi, C. Robertson, "Aligning arbitrary surfaces using pairwise geometric histograms", in: *Proc. Noblesse Workshop on Non-linear Model Based Image Analysis*, Glasgow, Scotland, 1998, pp. 103–108.
- [5] A. Ashbrook, R. Fisher, C. Robertson, N. Werghi, "Finding surface correspondence for object recognition and registration using pairwise geometric histograms", in: *Proc. European Conf. on Computer Vision*, 1998, pp. 674–686.
- [6] S.M. Yamany, A.A. Farag, "Free-form surface registration using surface signatures", in: *Int. Conf. on Computer Vision*, vol. 2, 1999, pp. 1098–1104.
- [7] D. Zhang, "Harmonic Shape Images: A 3D free-form surface representation and its applications in surface matching", Ph.D. thesis, Carnegie Mellon University, Pittsburgh, Pennsylvania 15213, USA (November 1999). M. Young, *The Technical Writers Handbook*. Mill Valley, CA: University Science, 1989.
- [8] C. Chua, R. Jarvis, Point signatures: a new representation for 3D object recognition, *Int. J. Comput. Vision* 25 (1) (1997) 63–85.
- [9] P. Krsek, T. Pajdla, V. Hlavac, R. Martin, "Range image registration driven by hierarchy of surface differential features", in: *Proc. 22nd Workshop of the Austrian Association for Pattern Recognition*, 1998, pp. 175–183.
- [10] A.J. Stoddart, K. Brunnstroem, Free-form surface matching using mean field theory, in: *British Machine Vision Conference*, Edinburgh, UK, 1996, pp. 33–42.
- [11] C. Chen, Y. Hung, RANSAC-Based DARCES: a new approach to fast automatic registration of partially overlapping range images, *IEEE Trans. Pattern Anal. Mach. Intell.* 21 (11) (1999) 1229–1234.
- [12] B.M. Planitz, A.J. Maeder, J.A. Williams, "The Correspondence Framework for 3D Surface Matching Algorithms", *Computer Vision and Image Understanding*, Volume 97, Issue 3, March 2005, pp 347-383.
- [13] A. Johnson, M. Hebert, "Surface registration by matching oriented points", in: *IEEE Proc. Int. Conf. on Recent Advances in 3-D Digital Imaging and Modeling*, 1997, pp. 121-128.
- [14] C. Torre-Ferrero, S. Robla, E.G. Sarabia, J.R. Llata, "CIRCON: An Alternative 3D Shape Representation for Surface Matching", *IECON'06, The 32nd Annual Conference of the IEEE Industrial Electronics Society*, Paris, France, 2006.